Contribution from the Department of Chemistry, University of Minnesota, Minneapolis, Minnesota 55455, and Science Research Laboratory, 3M Corporate Research Laboratories, St. Paul, Minnesota 55144

Electrochemistry and Infrared Spectroelectrochemistry of M_nSnPh_{4-n} (M = $CpMo(CO)_3$, $Mn(CO)_5$, $CpFe(CO)_2$; n = 1, 2)

John P. Bullock, Michael C. Palazzotto,[†] and Kent R. Mann*[,‡]

Received December 14, 1989

The electrochemistry and infrared spectroelectrochemistry of the series M_nSnPh_{4-n} (M = $CpMo(CO)_3$, $Mn(CO)_5$ and $CpFe(CO)_2$; n = 1, 2) and the corresponding homobinuclear compounds (M_2) were examined in CH_3CN/TBAH solutions (TBAH = tetra-*n*-butylammonium hexafluorophosphate). Cyclic voltammetric and double-potential step chroncoulometric data indicate that all of these compounds undergo net two-electron oxidations, with concomitant metal-tin or, in the case of the homobinuclear species, metal-metal bond rupture. The oxidation products for the triphenyltin adducts are the solvent adducts of the transition-metal cation and the triphenyltin cation. For $Mn(CO)_5SnPh_3$, the oxidation process is chemically reversible. Oxidation of the diphenyltin-bridged compounds results in cleavage of only one metal-tin bond, to give the metal cation and a base-stabilized stannylene cation. An ECE mechanism is proposed for the oxidation of these species. $[Mn(CO)_5]_3SnPh$ undergoes metal-tin bond cleavage reactions. The reductions of the compounds in this series and the homobinuclear compounds were also studied. Almost all of the reductions were net two-electron processes, which, like the oxidations, resulted in metal-tin or metal-metal bond cleavage. The reduction products for the homobinuclear species were the monomeric metal anions. The triphenyltin adducts yielded the metal anions and either the triphenylstannate anion or the triphenyltin dimer species, Sn_2Ph_6, upon reduction, depending on the transition-metal moiety. The diphenyltin-bridged compounds were reduced to the transition-metal anions and an unreduced tin product, possibly an oligomerization product of diphenyltin. Infrared spectral data imply that this reduction proceeds via a terminal diphenylstannate anion adduct of the transition-metal moiety.

Introduction

Organotransition-metal-tin chemistry has been an area of active research for nearly 3 decades. There have been several reviews published that deal extensively with the synthesis, reactivity, structure, and bonding of species within this large class of organometallic compounds.[1-6] The electrochemistry of these species, however, has received relatively little attention. This is surprising given the considerable interest in the electrochemical cleavage of metal-metal bonds.[7-23] In 1966, Dessy published a series of papers dealing with the electrochemistry of a wide variety of organometallic compounds,[7,8,24] among which were several organotin-transition-metal species. Since that time, only a few reports of the electrochemical behavior of these compounds have appeared. Several studies concerning the reduction of $CpFe(CO)_2SnPh_nCl_{3-n}$,[25-27] where n = 0, 1, 2, and 3, have been performed. For the case where n = 3, it was found that while the radical species $CpFe(CO)_2SnPh_3^-$ can be generated, it is unstable toward disproportionation, and on bulk electrolysis time scales, $CpFe(CO)_2SnPh_3$ undergoes a net two-electron reduction[28] with iron-tin bond cleavage. For species with tin-chlorine bonds, dimerization of the initially formed radicals was sometimes observed. Wrighton and co-workers found that compounds $R_3SnRe(CO)_3L$ (L = 1,10-phenanthroline, 2,2'-bipyridine, 2,2'-biquinoline; R = Ph, Me) undergo net two-electron oxidations that cleave the tin-rhenium bonds.[29] They also found that these species undergo reversible one-electron reductions; however, the reduction processes are thought to be primarily centered on the π^*L LUMO. Similarly, the compound (*meso*-tetrakis(4-methylphenyl)porphyrin)$SnFe(CO)_4$ was shown to undergo two reversible reductions via cyclic voltammetry; however, these reductions are also thought to primarily involve the porphyrin ring system rather than the iron-tin bond.[30]

This report describes a series of electrochemical and spectroelectrochemical experiments performed with the compounds M_nSnPh_{4-n} (M = $CpFe(CO)_2$, $Mn(CO)_5$ and $CpMo(CO)_3$; n = 1, 2), their transition-metal homobinuclear counterparts, M_2, and the related compounds $[Mn(CO)_5]_3SnPh$ and $[Mn(CO)_5]$-$SnPh_2[CpFe(CO)_2]$. We have examined both the oxidation and reduction processes these compounds undergo. Although the cyclic voltammetry of these compounds is quite similar, infrared spectroelectrochemical studies determined that a variety of electron-transfer products are generated upon their bulk electrolyses, and unambiguous identification of many of these species was accomplished with this technique.

Experimental Section

Synthesis. All syntheses were performed under a dinitrogen atmosphere by using standard Schlenk techniques. $[CpFe(CO)_2]_2$, $Mn_2(CO)_{10}$, and $[CpMo(CO)_3]_2$ were purchased from Pressure Chemical Co. and were used without further purification. $ClSnPh_3$ and Cl_2SnPh_2 were purchased from Aldrich and were used as received. Tetrahydrofuran was

* To whom correspondence should be addressed.
[†] 3M Corporate Research Laboratories.
[‡] University of Minnesota.

(1) Holt, M. S.; Wilson, W. L.; Nelson, J. H. *Chem. Rev.* **1989**, *89*, 11.
(2) Mackay, K. M.; Nicholson, B. K. *Comprehensive Organometallic Chemistry*; Pergamon Press: Oxford, England, 1982; Vol. 6, p 1043.
(3) Abel, E. W. *Comprehensive Inorganic Chemistry*; Pergamon Press: Oxford, 1973; Vol. 2, p 43.
(4) Brooks, E. H.; Cross, R. J. *Organomet. Chem. Rev.* **1970**, *6A*, 227.
(5) Donalson, J. D. *Prog. Inorg. Chem.* **1968**, *8*, 287.
(6) Vyazankin, N. S.; Razuvaev, G. A.; Krugkaya, O. A. *Organomet. Chem. Rev.* **1968**, *3A*, 323.
(7) Dessy, R. E.; Stary, F. E.; King, R. B.; Waldrop, M. *J. Am. Chem. Soc.* **1966**, *88*, 471.
(8) Dessy, R. E.; Weissman, P. M.; Pohl, R. L. *J. Am. Chem. Soc.* **1966**, *88*, 5117.
(9) Denisovich, L. I.; Ioganson, A. A.; Gubin, S. P.; Kolobova, N. E.; Anisimov, K. N. *Bull. Acad. Sci. USSR, Div. Chem. Sci. (Engl. Transl.)* **1969**, *18*, 218.
(10) Ferguson, J. A.; Meyer, T. J. *Inorg. Chem.* **1971**, *10*, 1025.
(11) Ferguson, J. A.; Meyer, T. J. *Inorg. Chem.* **1972**, *11*, 631.
(12) Pickett, C. J.; Pletcher, D. *J. Chem. Soc., Dalton Trans.* **1975**, 879.
(13) Meyer, T. J. *Prog. Inorg. Chem.* **1975**, *19*, 1.
(14) Lemoine, P.; Giraudeau, A.; Gross, M. *Electrochim. Acta* **1976**, *21*, 1.
(15) Lemoine, P.; Gross, M. *J. Organomet. Chem.* **1977**, *133*, 193.
(16) de Montauzon, D.; Poilblanc, R.; Lemoine, P.; Gross, M. *Electrochim. Acta* **1978**, *23*, 1247.
(17) Madach, T.; Vahrenkamp, H. *Z. Naturforsch., B: Anorg. Chem., Org. Chem.* **1979**, *34B*, 573.
(18) Miholova, D.; Vlcek, A. A. *Inorg. Chim. Acta* **1980**, *41*, 119.
(19) Legzdins, P.; Wassink, B. *Organometallics* **1984**, *3*, 1811.
(20) Connelly, N. G.; Geiger, W. E. *Adv. Organomet. Chem.* **1984**, *23*, 1.
(21) Lacombe, D. A.; Anderson, J. E.; Kadish, K. M. *Inorg. Chem.* **1986**, *25*, 2074.
(22) Kadish, K. M.; Lacombe, D. A.; Anderson, J. E. *Inorg. Chem.* **1986**, *25*, 2246.
(23) Jaitner, P.; Winder, W. *Inorg. Chim. Acta* **1987**, *128*, L17.
(24) (a) Dessy, R. E.; Pohl, R. L.; King, R. B. *J. Am. Chem. Soc.* **1966**, *88*, 5121. (b) Dessy, R. E.; Weissman, P. M. *J. Am. Chem. Soc.* **1966**, *88*, 5124. (c) Dessy, R. E.; Weissman, P. M. *J. Am. Chem. Soc.* **1966**, *88*, 5129.
(25) Miholová, D.; Vlcek, A. A. *Inorg. Chim. Acta* **1980**, *43*, 43.
(26) Miholová, D.; Vlcek, A. A. *Inorg. Chim. Acta* **1983**, *73*, 249.
(27) Combes, C.; Corriu, R. J. P.; Dabosi, G.; Henner, B. J. L.; Martineau, M. *J. Organomet. Chem.* **1984**, *270*, 141.
(28) Throughout this paper, references to "net two-electron" reduction or oxidation imply no mechanistic (i.e., ECE, EEC etc.) information. Only information concerning the reaction stoichiometry is conveyed.
(29) Luong, J. C.; Faltynek, R. A.; Wrighton, M. S. *J. Am. Chem. Soc.* **1980**, *102*, 7892.
(30) Kadish, K. M.; Boisselier-Cocolios, B.; Swistak, C.; Barbe, J. M.; Guilard, R. *Inorg. Chem.* **1986**, *25*, 121.

0020-1669/90/1329-4413$02.50/0

distilled from sodium/benzophenone under a dinitrogen atmosphere. $CpMo(CO)_3SnPh_3$,[31] $[CpMo(CO)_3]_2SnPh_2$,[32] $CpFe(CO)_2SnPh_3$,[33,34] $[CpFe(CO)_2]_2SnPh_2$,[35] $Mn(CO)_5SnPh_3$,[33] $[Mn(CO)_5]_2SnPh_2$,[33] and $[Mn(CO)_5]_3SnPh$[36] were prepared by slight modifications of literature methods, as described below for $CpFe(CO)_2SnPh_3$.

$CpFe(CO)_2SnPh_3$. The anion $CpFe(CO)_2^-$ was produced via the reduction of 3.0 g of $[CpFe(CO)_2]_2$ with 0.41 g of sodium and 0.50 g of benzophenone in 200 mL of THF. After conversion to the anion (about 24 h), 6.5 g of solid $ClSnPh_3$ was added, under argon, to the solution. The reaction was stirred until all of the anion was consumed, as monitored by infrared spectroscopy, at which time the solvent was removed under reduced pressure. The solid residue was taken up in methylene chloride and passed down a short silica gel column. The compound was purified by recrystallization from methylene chloride/heptane. The product was characterized by IR and ^1H NMR spectroscopy and elemental analysis.

Preparation of $[Mn(CO)_5]SnPh_2[CpFe(CO)_2]$.[37] This compound was prepared with minor modifications of the above procedure. Reactions were performed at −78 °C under dinitrogen. $CpFe(CO)_2^-$, which was generated by the reduction of $[CpFe(CO)_2]_2$ with sodium naphthalenide, was added to a solution of $ClSnPh_2Mn(CO)_5$[33,38] and stirred overnight. While being stirred, the solution was gradually warmed to room temperature. The yellow-orange product was purified by the above methods. IR (cm^{-1}): 2086 m, 1996 s, 1938 m. ^1H NMR (CD_3CN): δ 7.63 (m, aryl H, 4 H), 7.316 (m, aryl H, 6 H), 4.793 (s, Cp, 5 H).

Electrochemical Measurements. All electrochemical experiments were performed with a BAS 100 electrochemical analyzer unless otherwise noted.

Cyclic voltammetry (CV) and double-potential step chronocoulometry (CC) were performed at ambient temperature (25 °C) with a normal three-electrode configuration that consisted of a highly polished glassy-carbon disk working electrode (A = 0.07 cm^2), a AgCl/Ag reference electrode containing 1.0 M KCl, and a Pt auxilliary electrode. Bulk electrolyses were performed with a platinum-mesh electrode in place of the glassy-carbon electrode. The working compartment of the electrochemical cell was separated from the reference compartment by a modified Luggin capillary. All three compartments contained a 0.1 M solution of the supporting electrolyte.

The acetonitrile (Fisher) was distilled from P_2O_5 under a dinitrogen atmosphere. Methylene chloride (Burdick and Jackson) was dried over 4-Å molecular sieves. The supporting electrolyte, tetrabutylammonium hexafluorophosphate (TBAH) (Southwestern Analytical Chem., Inc.), was dried at 80 °C prior to use. In all cases working solutions were prepared by recording background cyclic voltammograms of the electrolyte solution before addition of the compound under study.[39] The working compartment of the cell was bubbled with solvent-saturated argon to deaerate the solution.

Potentials are reported vs aqueous AgCl/Ag and are not corrected for the junction potential. The standard current convention is used (anodic currents are negative). To allow future corrections and the correlation of these data with those of other workers, we have measured the $E°$ for the ferrocenium/ferrocene couple[40] under conditions identical with those used for the compounds under consideration. In CH_3CN/TBAH, $E°$ = 0.402 V; in CH_2Cl_2/TBAH, $E°$ = 0.460 V. No iR compensation was used.[41]

Double-potential step chronocoulometry experiments were used to determine $nD^{1/2}$ from the slope of Q vs $t^{1/2}$.[42] Potential steps were made from a point of no observable current to the diffusion plateau (determined from the cyclic voltammetry experiments). The step time was in the range of 250–500 ms. The value of n was chosen to give diffusion coefficients consistent with previous measurements of ferrocene solutions and to be consistent with the homobinuclear species $[CpFe(CO)_2]_2$ and $Mn_2(CO)_{10}$, both of which undergo net two electron oxidations and reductions in CH_3CN. A table of measured diffusion coefficients is included in the supplementary material.

Spectroelectrochemical Experiments. Infrared spectral changes during thin-layer bulk electrolyses were observed by using a flow-through spectroelectrochemical thin-layer cell as described previously.[43] Infrared data were collected on a Mattson Sirius 100 spectrometer. All IR data were corrected for a stray light error (13%) that originated from the inadvertant collection of light reflected off the front face of the CaF_2 plate of the spectroelectrochemical cell. Bulk electrolyses were controlled by an Electrosynthesis Co. (ESC) 410 potentiostatic controller and an ESC 420-A accessory power unit.

Table I. Cyclic Voltammetric Peak Potentials[a] (V vs Ag/AgCl) for the Oxidation and Reduction of Each of the Homobinuclear and Organotin Complexes Examined (in CH_3CN/TBAH)[b]

compound	E_a	E_c
$[CpMo(CO)_3]_2$	0.98	−0.99
$[CpMo(CO)_3]SnPh_3$	1.27, 1.39[c]	−1.86
$[CpMo(CO)_3]_2SnPh_2$	1.11	−1.50
$[Mn(CO)_5]_2$	1.47	−1.30
$[Mn(CO)_5]SnPh_3$	1.46	−2.01[d]
$[Mn(CO)_5]_2SnPh_2$	1.27	−1.83
$[Mn(CO)_5]_3SnPh$	1.44, 1.90[c]	−1.65
$[CpFe(CO)_2]_2$	0.61	−1.66
$[CpFe(CO)_2]SnPh_3$	1.13	−1.91[e]
$[CpFe(CO)_2]_2SnPh_2$	0.80	−2.00
$[Mn(CO)_5]SnPh_2[CpFe(CO)_2]$[f]	1.04	−1.80

[a] All E values listed are for electrode processes of bulk species. E values for coupled processes are discussed in the text. [b] Scan rate equals 250 mV/s unless otherwise noted. [c] See text. [d] Scan rate equals 100 mv/s. [e] Scan rate equals 500 mV/s. [f] The reduction of this compound was not studied in detail.

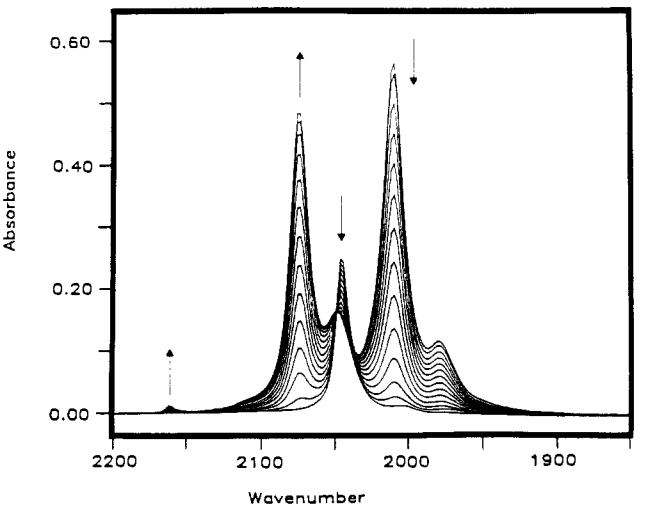

Figure 1. Infrared spectral changes observed upon oxidation of a 2.31 mM solution of $Mn_2(CO)_{10}$ in CH_3CN/TBAH at +1.80 V vs the Pt pseudoreference electrode in the thin-layer spectroelectrochemical cell. The peaks at 1980, 2010, and 2046 cm^{-1} decrease in intensity, while those due to $Mn(CO)_5(CH_3CN)^+$ at 2052, 2074 and 2160 cm^{-1} increase.

Results and Discussion

The oxidation and reduction potentials, as measured by cyclic voltammetry, for the series of substituted di- and triphenyltin–transition-metal species studied, are presented in Table I. Also included are data for the corresponding homobimetallic species, the trimanganese complex $[Mn(CO)_5]_3SnPh$, and the diphenyltin-bridged mixed-metal species $[Mn(CO)_5]SnPh_2[CpFe(CO)_2]$. Electrochemical data are available for the iron,[8,10,18,19] manga-

(31) Patil, H. R. H.; Graham, W. A. G. *Inorg. Chem.* **1966**, *5*, 1401.
(32) Struchkov, Yu. T.; Anisimov, K. N.; Osipova, O. P.; Kolobova, N. E.; Nesmeyanov, A. N. *Dokl. Akad. Nauk SSSR* **1967**, *172*, 107.
(33) Gorsich, R. D. *J. Am. Chem. Soc.* **1962**, *84*, 2486.
(34) Field, D. S.; Newlands, M. J. *J. Organomet. Chem.* **1971**, *27*, 213.
(35) Nesmeyanov, A. N.; Anisimov, K. N.; Kolobova, N. E.; Shirpkin, V. V. *Bull. Acad. Sci. USSr, Div. Chem. Sci.* **1966**, 1248.
(36) Thompson, J. A. J.; Graham, W. A. G. *Inorg. Chem.* **1967**, *10*, 1365.
(37) This species has also been synthesized by the reaction between $HSnPh_2[Mn(CO)_5]$ and $[CpFe(CO)_2]_2$; see: Collman, J. P.; Hoyano, J. K.; Murphy, D. W. *J. Am. Chem. Soc.* **1973**, *95*, 3424.
(38) Thompson, J. A. J.; Graham, W. A. G. *Inorg. Chem.* **1967**, *10*, 1875.
(39) Electrochemical experiments conducted with the light-sensitive compounds, notably $[CpMo(CO)_3]_2SnPh_2$, $[Mn(CO)_5]_3SnPh$, and $[CpFe(CO)_2]SnPh_2[Mn(CO)_5]$, were performed in the dark.
(40) Koepp, H. M.; Wendt, H.; Strehlow, H. Z. *Z. Elektrochem.* **1960**, *64*, 483.
(41) Gagne, R. R.; Koval, C. A.; Kisensky, G. C. *Inorg. Chem.* **1980**, *19*, 2854.
(42) Bard, A. J.; Faulkner, L. R. *Electrochemical Methods*; Wiley: New York, 1980; p 200.
(43) (a) Bullock, J. P.; Boyd, D. C.; Mann, K. R. *Inorg. Chem.* **1987**, *26*, 3084. (b) Bullock, J. P.; Mann, K. R. *Inorg. Chem.* **1989**, *28*, 4006.

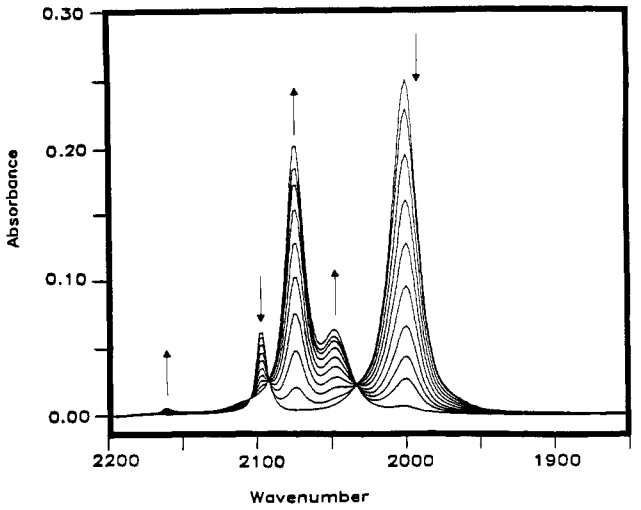

Figure 2. Infrared spectral changes observed during the electrooxidation of a 1.61 mM solution of $Mn(CO)_5SnPh_3$ at +2.05 V vs the Pt pseudo-reference electrode. The peaks due to the starting material, at 2000 and 2097 cm^{-1}, decrease in intensity while those for the product, $Mn(CO)_5(CH_3CN)^+$, increase.

nese,[8,9,12,14,15,21] and molybdenum[8,17,22,23] homobinuclear species and each of the triphenyltin adducts.[8,26] To our knowledge, there are no reports of the electrochemical behavior of the tin-bridged polynuclear species discussed in this work. Chronocoulometric experiments show that each of the oxidations and reductions are net two-electron processes, with the exceptions of the reductions of $CpFe(CO)_2SnPh_3$, $CpMo(CO)_3SnPh_3$, and $Mn(CO)_5SnPh_3$ (vide infra).

Oxidations. Homobinuclear Compounds. The diiron, dimanganese, and dimolybdenum species have all previously been studied by cyclic voltammetry, and our observations are in good agreement with the published results. In CH_3CN/TBAH, each of these compounds undergoes a net two-electron oxidation that cleaves the metal–metal bond to yield the monocationic acetonitrile adducts (eq 1).[12]

$$M_2 \xrightarrow{CH_3CN/TBAH} 2[M(CH_3CN)](PF_6) + 2e^- \quad (1)$$

$$M = CpFe(CO)_2,\ Mn(CO)_5,\ CpMo(CO)_3$$

Figure 1 shows the infrared spectroelectrochemical data collected during the electrolysis of $Mn_2(CO)_{10}$ to $Mn(CO)_5(CH_3CN)^+$. The maintenance of excellent isosbestic points throughout the electrolysis indicates that the conversion proceeds cleanly from the dimer to the monomer cations. Analogous experiments were performed with the diiron and dimolybdenum species, and each show similarly good isosbestic behavior.

Triphenyltin Adducts. The triphenyltin adducts of $CpFe(CO)_2$ and $Mn(CO)_5$, like their homobinuclear counterparts, undergo net two-electron oxidations that cleave the metal–tin bonds in each case. These electrooxidation processes yield two cationic metal species (eq 2): the transition-metal–acetonitrile adduct and a tin

$$MSnPh_3 \xrightarrow{CH_3CN} M(CH_3CN)^+ + Ph_3Sn(CH_3CN)_2^+ + 2e^- \quad (2)$$

$$M = CpFeCO_2,\ Mn(CO)_5$$

species, thought to be the solvated triphenyltin fragment $SnPh_3(CH_3CN)_2^+$ (the exact number of solvent molecules bound to the central tin ion is not clear; our designation of two bound acetonitriles, thereby yielding trigonal-bipyramidal geometry, is based on the known coordination chemistry of organotin halide compounds).[44]

Figure 2 presents the changes in the infrared spectrum that we observe during the electrooxidation of the tin–manganese complex.

(44) Harrison, P. G. *Comprehensive Coordination Chemistry*; Pergamon Press: Oxford, England, 1987; Vol. 3, p 183.

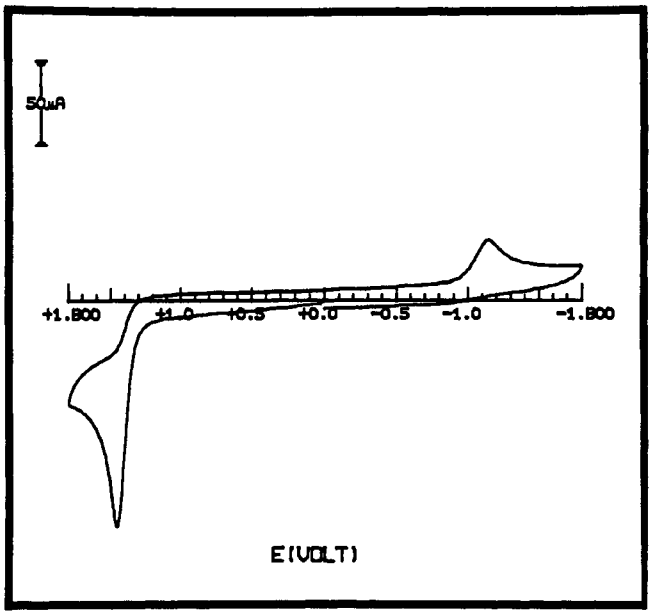

Figure 3. Cyclic voltammograms for a 1.61 mM solution of $Mn(CO)_5SnPh_3$ in CH_3CN/TBAH (scan rate = 250 mV/s). The scan was initiated in the positive direction. The potential is relative to a Ag/AgCl reference electrode.

The spectra show that $Mn(CO)_5SnPh_3$ is consumed as $Mn(CO)_5(CH_3CN)^+$ is isosbestically generated. With regards to the tin fragment, which is IR silent in this spectral region, evidence for the formation of a simple acetonitrile–tin adduct comes from additional cyclic voltammetric and IR spectroelectrochemical data. Figure 3 shows the cyclic voltammogram of $Mn(CO)_5SnPh_3$ in CH_3CN/TBAH; the scan was initiated in the positive direction. The voltammogram shows the net two-electron oxidation at 1.46 V relative to Ag/AgCl, and only one coupled cathodic return wave, at −1.14 V, is observed before the reduction wave of the starting compound (not shown) at −2.01 V. Chronocoulometric data (E_i = −1.80 V; E_f = 1.80 V) indicate hat the ratio of the charge passed in the forward step to the reverse step is 1; i.e., both forward and reverse processes involve net two-electron transfers. Moreover, after oxidation in the spectroelectrochemical thin cell followed by setting of the electrode potential negative of the return wave, approximately 95% of the starting material is regenerated. Thus, the redox chemistry of $Mn(CO)_5SnPh_3$ is chemically reversible.

The reduction process responsible for the cathodic return wave is due to the two-electron reduction of $Mn(CO)_5(CH_3CN)^+$ to give $Mn(CO)_5^-$. This was established by examination of the electrochemistry of $Mn(CO)_5(CH_3CN)^+$, which was generated via bulk electrolysis of $Mn_2(CO)_{10}$ in CH_3CN/TBAH (identification of the electrooxidation product was confirmed via infrared spectroscopy). This species exhibits a single, broad, reduction peak at −1.26 V (scan rate = 250 mV/s), and a return-coupled anodic peak at −0.14 V. We believe that the single reduction peak is due to the of conversion of $Mn(CO)_5(CH_3CN)^+$ to $Mn(CO)_5^-$ and that the return wave is due to the oxidation of the anion to $Mn_2(CO)_{10}$ (eqs 3 and 4). Our peak assignment for the initial

$$Mn(CO)_5(CH_3CN)^+ + 2e^- \rightarrow Mn(CO)_5^- \quad (3)$$

$$Mn(CO)_5^- \rightarrow \tfrac{1}{2}Mn_2(CO)_{10} + e^- \quad (4)$$

reduction wave differs from one given in the literature, which states that it is due to the one-electron reduction of the cation to give the neutral parent dimer.[21] Evidence in support of our interpretation of the cyclic voltammogram comes from double-potential step chronocoulometric data (E_i = 0.50 V; E_f = −1.70 V); this experiment shows that approximately twice the charge is passed in the forward step (reduction of $Mn(CO)_5(CH_3CN)^+$) relative to the charge passed in the reverse step. This is in accord with the predicted charge ratio expected for the above scheme. Moreover, the absence of a second reduction peak in the CV attributable to the neutral parent dimer is further evidence against

its formation by the reduction of $Mn(CO)_5(CH_3CN)^+$. The reduction of $Mn(CO)_5^+$ to $Mn(CO)_5^-$ in CH_2Cl_2/TBAP (TBAP = tetrabutylammonium perchlorate) has been observed by Kadish and co-workers.[21]

The electrochemistry of $Mn(CO)_5(CH_3CN)^+$ relates to the observed spectroelectrochemistry of the triphenyltin adduct of manganese pentacarbonyl because only one cathodic return wave due to the net two-electron-oxidation process is observed. The tin species remains in the solution at these potentials as the cationic acetonitrile adduct. Thus, the tine fragment is available to react with $Mn(CO)_5^-$ as it is formed by reduction at the electrode, to regenerate the starting compound (eqs 5 and 6). The reaction

$$Mn(CO)_5(CH_3CN)^+ + 2e^- \rightarrow [Mn(CO)_5]^- + CH_3CN \quad (5)$$

$$[Mn(CO)_5]^- + SnPh_3(CH_3CN)_2^+ \xrightarrow{fast} Mn(CO)_5SnPh_3 + 2CH_3CN \quad (6)$$

described by eq 6 must be fast on the thin-layer bulk electrolysis time scale because the conversion from the manganese cation to the tin–manganese adduct proceeds isosbestically. This reaction sequence nicely parallels the synthetic route to the manganese–tin adduct in which $Na[Mn(CO)_5]$ is reacted with Ph_3SnCl in a metathesis reaction; in the electrochemistry, the coordinated acetonitrile ligands act as the leaving groups from the tin center. This proposed scheme is also consistent with the known electrochemistry of $SnPh_3^+$; this species, with a perchlorate counterion, was generated by the metathesis of $ClSnPh_3$ with $AgClO_4$ and was reported to undergo reduction to $Ph_3Sn–SnPh_3$ at −1.6 V vs $Ag/AgClO_4$.[45] This potential is negative of the cathodic return wave for $Mn(CO)_5SnPh_3$; hence, no wave due to the tin fragment is seen as the tin cation is consumed by the reaction described by eq 6. Finally, we should note that there is a slight shift in the reduction potential of $Mn(CO)_5(CH_3CN)^+$ when $Ph_3Sn(CH_3CN)_2^+$ is in solution (from −1.26 to −1.14 V); this is likely due to a kinetic effect that arises from the rapid consumption of the generated anionic species in the following reaction (eq 6).

The chemical reversibility of the oxidation of $Mn(CO)_5SnPh_3$ is in contrast to the behavior of the analogous iron compound. The cyclic voltammogram of $CpFe(CO)_2SnPh_3$ exhibits an initial oxidation at 1.13 V that is coupled to a return cathodic peak at −0.61 V. On the basis of the observed return peak potential, the coupled reduction process was assigned to the reduction of electrogenerated $CpFe(CO)_2(CH_3CN)^+$ to $[CpFe(CO)_2]_2$;[46] this assignment was confirmed by spectroelectrochemical data. Thus, the pathway to regenerating the iron–tin complex, that is, reaction between electrogenerated metal anion and triphenyltin cation (the iron analogue of eq 6) is unavailable in this case, and subsequently, the oxidation process is chemically irreversible.

The oxidation chemistry of the molybdenum analogue is not as simple as it is in the iron and manganese systems. In this case, the cyclic voltammogram shows two very closely spaced anodic processes. The initial process is a net two-electron oxidation analogous to that described by eq 2, whereas the second process appears to involve further oxidation of the electrochemically generated $CpMo(CO)_3(CH_3CN)^+$ fragment. The second process is also observed in the cyclic voltammogram of the homonuclear molybdenum dimer. Spectroelectrochemical data for this compound show a clean, isosbestic conversion of the dimer to the cationic monomer but only in the beginning of the electrolysis. Reasonable isosbestic points are maintained until approximately 80% of the starting material has been consumed (about 50 s after the start of electrolysis). After this time, the consumption of the acetonitrile adduct becomes noticeable and the isosbestic behavior is lost. The final oxidation product does not exhibit an easily interpretable IR spectrum and has not been identified.

Polynuclear Species. Compounds with organotin bridging ligands (M_2SnPh_2) also undergo net two-electron oxidations in CH_3CN/TBAH. For the dimanganese and dimolybdenum tin-bridged species, these oxidations proceed cleanly as evidenced by the maintainence of isosbestic points in the spectroelectrochemical data. Figure 4 illustrates the spectral changes observed during the oxidation of the manganese complex. Examination of the spectrum taken after the completion of the oxidation reveals the presence of two manganese carbonyl species, one of which is $Mn(CO)_5(CH_3CN)^+$. The other species has an infrared spectrum which is similar to that of $Mn(CO)_5SnPh_3$ with regards to the number of peaks and the ratio of peak heights; i.e., both spectra show a sharp, low-intensity peak at high energy and a much larger, broader peak approximately 95 cm^{-1} lower in energy. However, the peaks of the oxidation product are higher in energy by about 20 cm^{-1} compared to the analogous peaks of the triphenyltin adduct. This IR peak pattern is often seen for monosubstituted pseudooctahedral $M(CO)_5L$ species (C_{4v} symmetry), with the higher energy peak corresponding to one of the two A_1 modes and the larger peak being due to the overlap of the second A_1 mode and the E mode.[47] This information leads us to assign the other oxidation product as the cationic, base-stabilized (diarylstannylene)manganese species, $Mn(CO)_5SnPh_2(CH_3CN)_2^+$. Similar base-stabilized stannylenes have been synthesized chemically and have been widely reported.[1] This is, however, the first example to our knowledge of the electrochemical generation of this type of compound. The generation of the stannylene species is not unique to the electrooxidation of the dimanganese compound either, as analogous species were oberved upon oxidation of the tin-bridged diiron and dimolybdenum compounds as well. Table II presents the IR stretching frequencies for each of the base-stabilized stannylene complexes observed, along with those for the corresponding triphenyltin adducts and the acetonitrile adduct cations, as well as additional data to be discussed later.

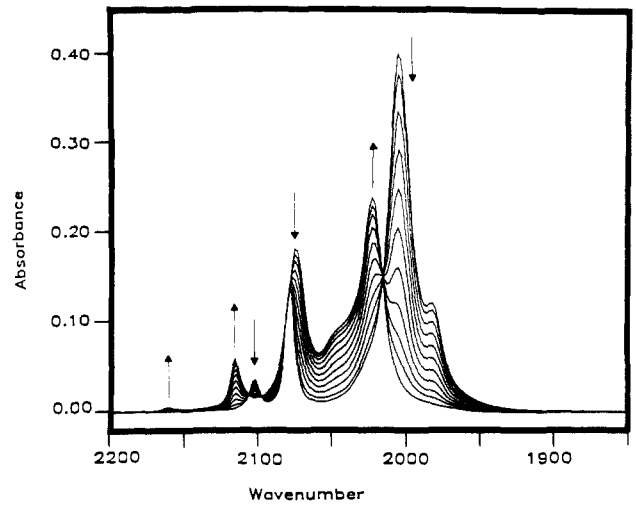

Figure 4. Infrared spectral changes observed upon oxidation of a 1.67 mM solution of $[Mn(CO)_5]_2SnPh_2$ at +1.80 V vs the Pt pseudo-reference electrode. The initial peaks at 1983, 2006, 2079 and 2103 cm^{-1} decrease in intensity as the peaks for $Mn(CO)_5(CH_3CN)^+$ and $Mn(CO)_5SnPh_2(CH_3CN)_2^+$ (ν_{CO} = 2116, 2023 cm^{-1}) grow in.

Thus, the behavior of these compounds when oxidized can be described as cleavage of one of the tin–metal bonds to form the metal–acetonitrile adduct cation and the base-stabilized stannylene cation (eq 7).

$$Ph_2SnM_2 \xrightarrow{CH_3CN} MSnPh_2(CH_3CN)_2^+ + M(CH_3CN)^+ + 2e^- \quad (7)$$

$$M = CpMo(CO)_3,\ Mn(CO)_5,\ CpFe(CO)_2$$

Attempts to generate the base-stabilized manganese–stannylene compound via the reaction of $AgPF_6$ with $ClPh_2SnMn(CO)_5$ in acetonitrile were unsuccessful; no AgCl precipitated from solution, and the infrared spectrum of the reaction mixture showed no change from that of the starting material. This behavior sharply

(45) Dessy, R. E.; Kitching, W.; Chivers, T. *J. Am. Chem. Soc.* **1966**, *88*, 453.
(46) Bullock, J. P.; Mann, K. R. Work in progress.
(47) Ugo, R.; Cenini, S.; Bonati, F. *Inorg. Chim. Acta* **1967**, *1*, 451.

Table II. Infrared CO Stretching Frequencies (in cm^{-1}) of ML^n Complexes

M	L = CH_3CN; $n = +1$	L = $SnPh_2(CH_3CN)$; $n = +1$	L = $SnPh_3$; $n = 0$	L = $SnPh_2^-$;[a] $n = -1$	L = 2 e^-;[b] $n = -1$
$CpMo(CO)_3$	2075	2030	2002	*c*	1896
	1991	1961	1926		1776
		1936	1899		
$Mn(CO)_5$	2160	2116	2097	*c*	1901
	2074	2023	2000		1863
	2052				
$CpFe(CO)_2$	2078	2018	1991	1961	1862
	2034	1972	1940	1907	1787

[a] See text. [b] This designation refers to the 18-e^- metal anion. [c] Not observed.

contrasts with the behavior of $ClSnPh_3$ in the presence of Ag^+ (vide supra); when $AgPF_6$ is introduced to an acetonitrile solution of $ClSnPh_3$, AgCl immediately precipitates from solution, and the acetonitrile-solvated triphenyltin cation is generated. The inability of Ag^+ to abstract Cl^- from the tin center indicates that the tin–chlorine bond is quite strong and, further, implies that the electrogenerated stannylene species is strongly Lewis acidic. The ability of stannylenes to act simultaneously as Lewis bases, in this case toward manganese pentacarbonyl, and as Lewis acids, has been commented on by other workers.[1]

The stabilizing influence of the base on the stannylene species is demonstrated when a tin-bridged species is oxidized in a noncoordinating solvent/electrolyte. For example, oxidation of $[CpMo(CO)_3]_2SnPh_2$ in acetonitrile results in an isosbestic conversion to the acetonitrile-stabilized stannylene and $CpMo(CO)_3(CH_3CN)^+$; no decomposition of these products is observed. However, when the same compound was oxidized in CH_2Cl_2/TBAH, the initial products generated are analogous to those generated in acetonitrile, i.e., the stannylene and the molybdenum cation fragment, but are not stable.[48] When the only species available to coordinate to the stannylene are CH_2Cl_2 and PF_6^-, which are both much weaker Lewis bases than acetonitrile, the stannylene is stabilized to a lesser extent and decomposes as a result. This observation is consistent with a report by Marks in which attempts to remove the bases from other base-stabilized metal carbonyl–stannylene compounds, or attempts to synthesize the stannylenes in noncoordinating solvents, resulted in decomposition rather than stannylene formation.[50]

On the basis of the spectroelectrochemical data, eq 7 adequately describes the electrochemistry of the diphenyltin-bridged dimanganese and dimolybdenum compounds; however, the oxidation process of the analogous diiron species is more complex. Early in the electrolysis (about the first 10 s) of $[CpFe(CO)_2]_2SnPh_2$, an isosbestic point is seen as the complex is consumed to form $CpFe(CO)_2(CH_3CN)^+$ and another species (ν_{CO} 1959, 2008 cm^-); however, the isosbestic point is lost as the final iron–tin species (the base-stabilized stannylene complex) begins to grow in. The nature of the intermediate complex is unknown. The possibility that the intermediate is, in fact, the stannylene analogue to those observed in the manganese and molybdenum systems is unlikely given the peak positions relative to the triphenyltin adduct of $CpFe(CO)_2$; the peaks for the intermediate are an average of 18 cm^{-1} higher in energy than those for the triphenyltin adduct. This

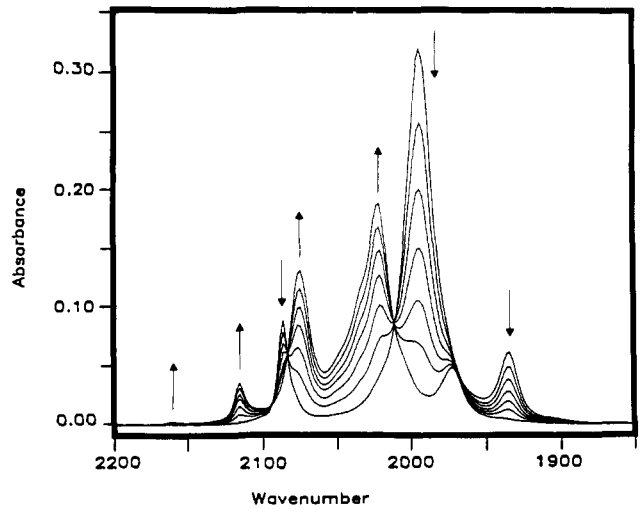

Figure 5. Infrared spectral changes observed during electrooxidation of a 1.94 mM solution of $[Mn(CO)_5]SnPh_2[CpFe(CO)_2]$ at +1.60 V vs the Pt pseudoreference electrode. The peaks due to the starting material at 1938, 1996, and 2086 cm^{-1} decrease as peaks due to the four electrogenerated species grow in.

compares to 21 cm^{-1} for the difference between the triphenyltin adduct and stannylene complex of $Mn(CO)_5$, and 33 cm^{-1} for the analogous $CpMo(CO)_3$ complexes. Due to the much greater electron-withdrawing ability of the carbonyl ligand relative to cyclopentadienyl and a similar expectation for $Ph_2Sn(CH_3CN)_2^+$ relative to Ph_3Sn, the shifts in stretching frequencies between the base-stabilized stannylenes and the triphenyltin adducts would be greater for the cyclopentadienyl-substituted metals than for manganese pentacarbonyl. The difference between the IR bands in what is thought to be the stannylene complex and the triphenyltin adduct of $CpFe(CO)_2$ is 30 cm^{-1}, very similar to the difference of 33 cm^{-1} observed for the analogous $CpMo(CO)_3$ species.

Perhaps the most interesting electrochemistry we have observed arises from the mixed-metal tin-bridged species $[CpFe(CO)_2]SnPh_2[Mn(CO)_5]$. In some respects, it behaves similarly to the other tin-bridged species in that it exhibits an net two-electron oxidation. A comparison of the cyclic voltammograms of the tin-bridged diiron, dimanganese, and iron–manganese compounds reveals two interesting features.[51] First, the oxidation potential of the mixed-metal compound is at an intermediate potential relative to those for the diiron and dimanganese species (see Table I). This implies that the molecular orbital from which the electron is removed in the initial electron-transfer step (vide infra) has large contributions from both the iron and manganese moieties. Second, the cathodic return of the mixed-metal species shows two major peaks at −0.66 and −1.13 V, which are coupled to the initial oxidation. The diiron complex also shows two coupled peaks, at −0.67 and −1.12 V, due to the reduction of electrogenerated $CpFe(CO)_2(CH_3CN)^+$ and, presumably, the iron base-stabilized stannylene cation, respectively. The dimanganese compound exhibits a single coupled return peak at −1.14 V, due to the reduction of $Mn(CO)_5(CH_3CN)^+$. The potentials of the coupled reduction peaks for the mixed-metal compound imply that both $CpFe(CO)_2(CH_3CN)^+$ and $Mn(CO)_5(CH_3CN)^+$ are generated by the initial oxidation step; however, the close proximity of the iron–stannylene reduction to that of $Mn(CO)_5(CH_3CN)^+$ makes the assignment of the second coupled reduction peak of the mixed-metal compound ambiguous based on only the CV data. Infrared spectroelectrochemical data accompanying the oxidation (Figure 5) clarify the cyclic voltammetric information as it shows that both the iron and manganese stannylenes, as well as the iron and manganese cations, are generated upon electrooxidation of the mixed-metal complex. The spectral changes proceed isosbestically, indicating that the generation of products proceeds at

(48) Oxidation of $[CpMo(CO)_3]_2SnPh_2$ in CH_2Cl_2/TBAH (E_a = 1.21 V) is more complicated than in CH_3CN; at the beginning of the electrolysis, an intermediate is observed with IR peaks at 2018, 1949, and 1919 cm^{-1}; these are similar to peaks observed if the electrolysis is stopped before completion, that is, if the stannylene is allowed to decompose in solution without the application of an oxidizing potential at the electrode. This may indicate the existence of an equilibrium between the stannylene and a less highly oxidized species. The intermediate, however, is soon consumed during the electrolysis, as the stannylene (ν_{CO} = 2034, 1969 (sh), 1931 cm^{-1}) increases in concentration. $CpMo(CO)_3(PF_6)$[49] is also generated during the electrolysis; however, it decomposes as well.

(49) Beck, W.; Scholter, K. *Z. Naturforsch., B: Anorg. Chem., Org. Chem.* **1978**, *33B*, 1214.

(50) Marks, T. J. *J. Am. Chem. Soc.* **1971**, *93*, 7090.

(51) A figure is shown in the supplementary material.

Scheme I

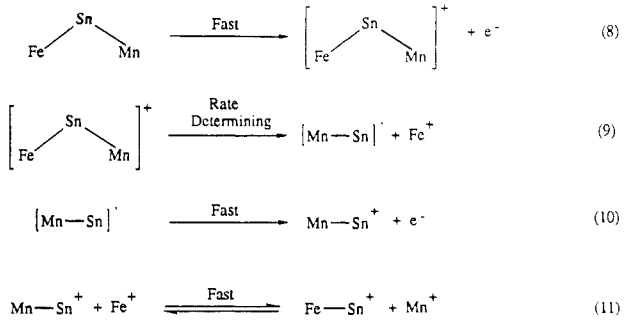

(8) (9) (10) (11)

Scheme II

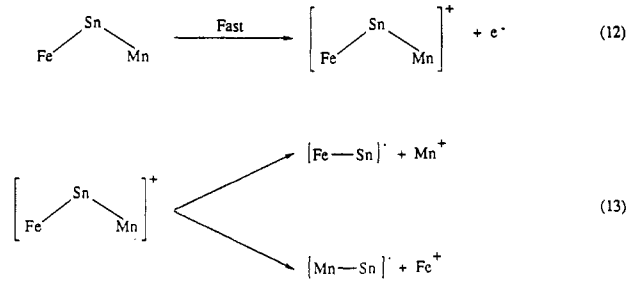

(12) (13) (14) (15)

Scheme III

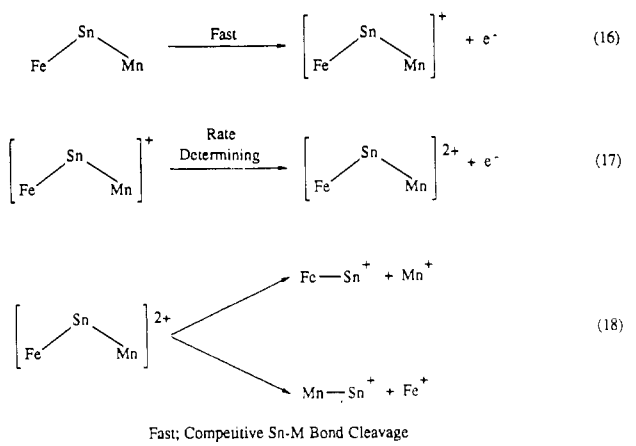

(16) (17) (18)

a constant ratio throughout the electrolysis. At the completion of the electrolysis, roughly equimolar amounts of $CpFe(CO)_2(CH_3CN)^+$, $Mn(CO)_5(CH_3CN)^+$, $CpFe(CO)_2SnPh_2(CH_3CN)_2^+$, and $Mn(CO)_5SnPh_2(CH_3CN)_2^+$ are present,[52] based on the absolute integrated intensities for each of the components (determined in other experiments).

We consider three possible explanations for the generation of both the iron and manganese stannylene complexes (Schemes I–III). One is that there is a single ECE route leading directly to only two of the observed products, followed by a rapid equilibrium between the electrogenerated products that gives rise to the other two observed species (Scheme I). A second ECE mechanism is considered in which there are two separate chemical reactions between the first and second electron transfers (Scheme II). Finally, we examine an EEC mechanism that involves two different chemical reactions after both electrons are transferred from the starting compound (Scheme III).

(52) A small amount of an unknown compound, probably a $CpFe(CO)_2L$ species on the basis of the IR peak pattern, was also generated during the electrolysis; approximately 93% of the total integrated area under the final spectrum in the series is made up of the four known components.

Table III. Values of $[E_p - E_{p/2}]$ (mV) for the Oxidation of Several Diphenyltin-Bridged and Homobinuclear Compounds[a]

compound	$(E_p - E_{p/2})$
$[Mn(CO)_5]_2$	74
$[CpFe(CO)_2]_2$	108
$[Mn(CO)_5]_2SnPh_2$	86
$[CpFe(CO)_2]_2SnPh_2$	91
$[Mn(CO)_5]SnPh_2[CpFe(CO)_2]$	77

[a] Measured at a scan rate of 100 mV/s in CH_3CN/TBAH.

In Scheme I (eqs 8–11), an initial one-electron transfer generates a diphenyltin-bridged radical cationic species that rapidly undergoes cleavage of one of the tin–metal bonds, either the tin–manganese or the tin–iron bond, to form the metal cation and a tin radical.[29] The tin radical is then oxidized at the electrode to yield the stannylene species. The generation of the second stannylene is accomplished via a rapid equilibrium between the metal cation species and the initially formed stannylene. For example, if the tin–iron bond were the bond to be cleaved in the ECE mechanism, as is shown in eq 9 (the tin–manganese bond could also be the one which breaks), the resulting products, $CpFe(CO)_2(CH_3CN)^+$ and $Mn(CO)_5SnPh_2(CH_3CN)_2^+$, could then be involved in an equilibrium to generate the complementary species, $Mn(CO)_5(CH_3CN)^+$ and $CpFe(CO)_2SnPh_2(CH_3CN)_2^+$. The presence of isosbestic points in the spectroelectrochemical data require that this equilibrium be rapid on this time scale. To test for the existence of this equilibrium, the diphenyltin-bridged dimanganese complex was oxidized in the presence of $CpFe(CO)_2(CH_3CN)^+$ (generated via exhaustive bulk electrolysis of the parent dimer in CH_3CN/TBAH at +0.9 V vs Ag/AgCl). The presence of an equilibrium similar to that described in eq 11 would result in the formation of the iron stannylene upon oxidation of the manganese compound. Infrared data show conclusively that the oxidation only generates $Mn(CO)_5(CH_3CN)^+$ and the manganese stannylene, the same products generated when no iron was present in solution. Thus Scheme I is eliminated as a possible mechanism.

Scheme II (eqs 12–15), like Scheme I, is an ECE mechanism. However, this mechanism allows for two competing chemical reactions between the transfer of the first and second electrons. That is, the initial oxidation process is delocalized over both tin–metal bonds (i.e., the HOMO has significant contributions from the iron and manganese fragments) and weakens both of them as a result. The relative amounts of the manganese–tin and iron–tin radicals are kinetically controlled by competitive bond cleavage of either the iron–tin or the manganese–tin bond, respectively. The ratio of the two processes is a function of the relative bond strengths in the iron–tin–manganese cation-radical species. The final electron transfer is simply the nonselective oxidation of the kinetically controlled mixture of the iron–tin and manganese–tin radical species (eqs 14 and 15).

The final mechanism to be considered, shown in Scheme III (eqs 16–18), is an EEC mechanism. In this sequence, an initial electron-transfer step generates the polynuclear radical-cation intermediate; this step is followed by a second electron transfer prior to the cleavage of a tin–metal bond. After the second electron is transferred, the resulting dication undergoes two competing reactions, one that cleaves the iron–tin bond and another that cleaves the manganese–tin bond. These reactions are entirely analogous to those illustrated in eq 13 in Scheme II; they differ only in that in this case the bond cleavages occur after the second electron is transferred, whereas in Scheme II, they occur prior to the second electron-transfer.

Both schemes II and III are consistent with both our infrared spectroelectrochemical data and our electrochemical data. For example, the peak widths of the cyclic voltammograms are consistent with mechanisms involving initial one-electron-transfer steps. Specifically, the $[E_p - E_{p/2}]$ value for the mixed-metal

compound, 77 mV, is inconsistent with a diffusion-controlled two-electron-transfer process.[53] Table III shows the $[E_p - E_{p/2}]$ values for this compound, the diphenyltin-bridged homonuclear species, and the homobinuclear iron and manganese compounds. These are all much larger than the theoretical values of 30 mV for diffusion-controlled two-electron processes and are more consistent with mechanisms involving initial one-electron transfers. While we cannot rule out the possibility of an EEC mechanism (Scheme III), we favor the ECE mechanism (Scheme II) based on the chemistry of similar systems. For example, there is considerable evidence that $[Mn(CO)_5]_2$,[21] $[CpMo(CO)_3]_2$,[22] and $[CpFe(CO)_2]_2$,[46] while they undergo net two-electron transfers, do so via ECE mechanisms.[54]

The final oxidation processes studied were those for the trimanganese complex, $[Mn(CO)_5]_3SnPh$. Unlike the previous compounds discussed, this species exhibits two net two-electron oxidations in CH_3CN/TBAH at 1.44 and 1.90 V. A single coupled cathodic peak is observed at −1.16 V, the current of which decreases significantly if the sweep direction is reversed between the two oxidation peaks instead of performing both processes. This information is strong evidence that both oxidation processes generate a common product, which, on the basis of the measured reduction potential, is assigned as $Mn(CO)_5(CH_3CN)^+$. Thus, $[Mn(CO)_5]_3SnPh$ is thought to undergo sequential cleavage of tin–manganese bonds as the applied potential is made more positive (eqs 19 and 20). The tin product of the first oxidation, $[Mn(CO)_5]_2SnPh(CH_3CN)_2^+$, is isoelectronic with the base-stabilized stannylenes generated upon oxidation of the diphenyltin-bridging compounds, with one of the organic moieties replaced by an organometallic fragment. Further oxidation of the tin species yields the dication $Mn(CO)_5SnPh(CH_3CN)_3^{2+}$. This compound is also isoelectronic with the base-stabilized stannylenes; however, in this case, one of the phenyl rings is substituted by an additional acetonitrile molecule. Spectroscopic evidence for the generation of both of these oxidation products was obtained via infrared spectroelectrochemical experiments. Upon oxidation of the trimanganese–tin compound at a potential inbetween those of the two anodic peaks observed on the cyclic voltammogram, isosbestic behavior[51] is seen only in the beginning of the electrolysis as the neutral starting material is consumed to yield the products described by eq 19. The isosbestic point is lost as the initial oxidation product, $[Mn(CO)_5]_2SnPh(CH_3CN)_2^+$, is consumed in the second oxidation product, $[Mn(CO)_5]_2SnPh(CH_3CN)_2^+$, is consumed in the second oxidation process (eq 20) before all of the starting compound is depleted. It is not clear whether or not the isosbestic point was lost due to an overlap of the oxidation peaks, such that both oxidations can occur simultaneously, or to a disproportionation reaction of the initial oxidation product. An isosbestic point is reestablished after all of $[Mn(CO)_5]_3SnPh$ is consumed, at which point only the second oxidation process occurs in solution.

$$[Mn(CO)_5]_3SnPh \xrightarrow{CH_3CN} [Mn(CO)_5]_2SnPh(CH_3CN)_2^+ + Mn(CO)_5(CH_3CN)^+ + 2e^- \quad (19)$$

$$[Mn(CO)_5]_2SnPh(CH_3CN)_2^+ \xrightarrow{CH_3CN} Mn(CO)_5SnPh(CH_3CN)_3^{2+} + Mn(CO)_5(CH_3CN)^+ + 2e^- \quad (20)$$

The carbonyl stretching frequencies and ratio of peak heights observed for the oxidation products are consistent with our product assignments. For example, the species assigned as $Mn(CO)_5SnPh(CH_3CN)_3^{2+}$ (ν_{CO} 2127, 2037 cm^{-1}) exhibits an infrared spectrum similar to those of $Mn(CO)_5SnPh_3$ and $Mn(CO)_5SnPh_2(CH_3CN)_2^+$ with respect to the peak height ratios (vide supra). Moreover, the stretching frequencies for the dication are an average of 13 cm^{-1} higher in energy compared to those for the base-stabilized manganese stannylene monocation and 34 cm^{-1} higher than those for the neutral manganese-triphenyltin adduct. Likewise, $[Mn(CO)_5]_2SnPh(CH_3CN)_2^+$ (ν_{CO} 2122, 2095, 2028 cm^{-1}) shows a peak pattern similar to that seen for the diphenyltin-bridged dimanganese compound at an average of 19 cm^{-1} higher in energy. These peak shifts are too small to be explained by a formal change in the manganese oxidation state but are in accord with expected shifts based on the differences in electron-withdrawing abilities of the tin fragments.

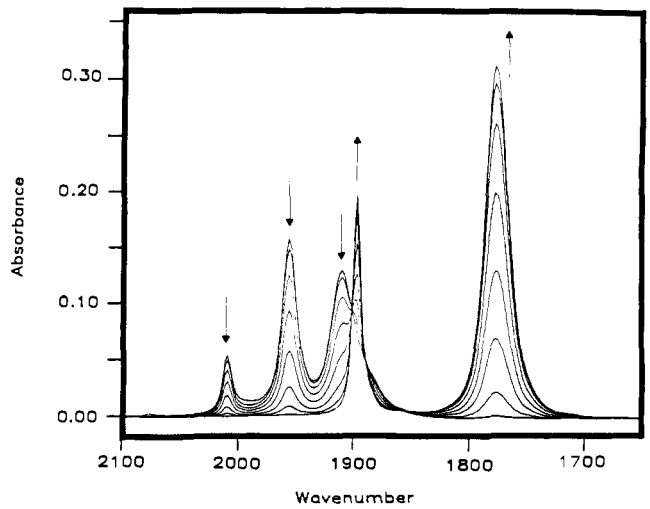

Figure 6. Infrared spectral changes observed during the reduction of a 1.72 mM solution of $[CpMo(CO)_3]_2$ at −1.50 V vs the Pt pseudoreference electrode. The peaks at 1909, 1955, and 2009 cm^{-1} decrease in intensity while those due to the product, $[CpMo(CO)_3]^-$, at 1776 and 1896 cm^{-1} increase.

Reductions. Homobinuclear Compounds. The reduction of each of the homobinuclear compounds under study has been examined via cyclic voltammetry in earlier works.[18,21,22] In each case, net two-electron reductions are seen, and it is well established that these reductions yield the corresponding 18-electron monoanionic fragments. Our infrared spectroelectrochemical experiments are in accord with these previous results. Figure 6 shows the spectral changes that accompany the reduction of $[CpMo(CO)_3]_2$ in CH_3CN/TBAH. The net reductions are described by eq 21.

$$M_2 + 2e^- \rightarrow 2M^- \quad (21)$$

$$M = CpFe(CO)_3,\ Mn(CO)_5,\ CpMo(CO)_3$$

Organotin Adducts. Each of the three triphenyltin adducts studied were previously examined by polarography by Dessy and co-workers, albeit with a dropping mercury electrode.[8] In this earlier work, it was reported that each of these species undergo one-electron reductions to yield the organometallic anion and triphenyltin radical, which couples to give Sn_2Ph_6. Except for the reduction of $CpMo(CO)_3SnPh_3$, we observed significantly different results than those of Dessy. Reduction of the molybdenum–tin compound in the IR spectroelectrochemical thin cell proceeds cleanly,[51] as is evidenced by sharp isosbestic points, and yields the products reported by Dessy (eq 22). The electrochemical data (i.e., CV and CC experiments) of the iron–tin and manganese–tin reductions are more consistent with net two-electron processes than with the one-electron process observed for the molybdenum species. Our observations concerning the reduction of the iron–tin species are in good agreement with those of Miholová and Vlcek[26] discussed below.

$$CpMo(CO)_3SnPh_3 + e^- \rightarrow CpMo(CO)_3^- + Sn_2Ph_6 \quad (22)$$

They studied the polarographic reduction of $CpFe(CO)_2SnPh_3$ in THF/TBAP and reported the presence of two reduction waves ($E_{1/2}$ = −1.86 and −2.21 V vs SCE), both of which are due to one-electron processes. Cyclic voltammetry at a platinum electrode showed that the first process is reversible electrochemically but

(53) (a) Nicholson, R. S.; Shain, I. *Anal. Chem.* **1964**, *36*, 406; (b) Nicholson, R. S.; Shain, I. *Anal. Chem.* **1965**, *37*, 178.

(54) While the oxidation of $Mn_2(CO)_{10}$ is believed to proceed via an ECE mechanism, with a diffusion-controlled initial electron-transfer step,[21] the large value of $[E_p - E_{p/2}]$ for $[CpFe(CO)_2]_2$ indicates the mechanism involves a slow electron-transfer; i.e., it has a different rate-determining step.

that the electrogenerated species is consumed in a subsequent chemical reaction. The initial formed radical species, $CpFe(CO)_2SnPh_3^-$, is thought to decompose via a disproportionation reaction to the neutral parent species and the anionic fragments $SnPh_3^-$ and $CpFe(CO)_2^-$. The identity of the final reduced species was confirmed by IR and UV–vis spectroscopy of a solution that had undergone exhaustive electrolysis performed at the first reduction potential. In CH_3CN/TBAH, we observed a quasireversible reduction at −1.91 vs Ag/AgCl (scan rate = 500 mV/s), but the peak current of the return oxidation wave was highly dependent on scan rate. At 40 mV/s, the reduction wave showed almost no return current. We also observe a second scan-rate-dependent reduction wave at −2.40 V, with the current, relative to the first reduction wave, larger at higher scan rates. These observations are consistent with the disproportionation scheme outlined above. Reduction of $CpFe(CO)_2SnPh_3$ in the IR cell[51] showed that the conversion from the tin adduct to the iron anionic species proceeds isobestically, indicating that the concentration of the radical species is never high enough to be observed via infrared spectroscopy during the electrolysis; i.e., at room temperature the disproportionation occurs too fast for the intermediate to be observed on the thin-cell bulk electrolysis time scale. This result is in accord with additional observations made by Miholová and Vlcek that the EPR spectrum of the in situ electrochemically generated radical species was not observed at room temperature but *was* observed at −20 °C.

We observe a second anodic return wave at −0.92 V coupled to the reduction of $CpFe(CO)_2SnPh_3$ and assign it to the net one-electron oxidation of $CpFe(CO)_2^-$ to the neutral parent dimer.[46] However, the infrared spectral changes that accompany this anodic process do *not* show the generation of $[CpFe(CO)_2]_2$ but rather the regeneration of the iron–tin starting compound. Dessy has studied the reactions of organometallic anions with metal–metal-bonded compounds and found that if $[CpFe(CO)_2]_2$ is reacted with $SnPh_3^-$, the produces are the iron–tin adduct and $CpFe(CO)_2^-$.[24b] Thus the starting compound is regenerated via chemical reactions that follow the electron transfer but produces the anodic wave (eqs 23 and 24).

$$CpFe(CO)_2^- \rightarrow \tfrac{1}{2}[CpFe(CO)_2]_2 + e^- \quad (23)$$

$$[CpFe(CO)_2]_2 + 2SnPh_3^- \rightarrow 2CpFe(CO)_2SnPh_3 \quad (24)$$

This chemistry nicely parallels the chemically reversible oxidation chemistry of $Mn(CO)_5SnPh_3$. The peak separations for the reduction of the iron–tin compound and its return peak, as well as that for the oxidation of the manganese–tin species and its return, are quite large, about 1.0 and 2.5 V, respectively, but in each case the starting compounds are each regenerated in the return sweeps; i.e., they are both chemically reversible.

Reduction of $Mn(CO)_5SnPh_3$ appears to be a net two-electron process that yields primarily $Mn(CO)_5^-$ and $SnPh_3^-$, but a small amount of an unidentified compound (ν_{CO} 1906, 1995 cm^{-1}) is also generated during the reduction. The nature of the minor product and the pathway for its formation were not studied.

The reductions of the diphenyltin-bridged species were also studied. Each of these compounds undergoes a net two-electron reduction. This is in agreement with an observation made by Dessy concerning the reduction of the closely related species $[CpMo(CO)_3]_2SnMe_2$.[8] This compound undergoes a net two-electron reduction to yield 2 equiv of $CpMo(CO)_3^-$ and a neutral, oligomeric tin species, $(SnMe_2)_n$. Reduction of $[CpMo(CO)_3]_2SnPh_2$ in the IR spectroelectrochemical cell shows[51] an isosbestic conversion to 2 equiv of $CpMo(CO)_3^-$, in accord with Dessy's results. Similarly, the tin product is thought to be an oligomer, $(SnPh_2)_n$ (eq 25).[55] Bulk electrolysis of the analogous iron compound at

$$[CpMo(CO)_3]_2SnPh_2 + 2e^- \rightarrow 2[CpMo(CO)_3]^- + (1/n)[SnPh_2]_n \quad (25)$$

−2.2 V confirms that the overall reduction is a two-electron process and indicates that the tin species generated undergoes no net reduction during the reaction.

As mentioned above, reduction of the diphenyltin-bridged iron analogue is also a net two-electron process, but unlike the case of molybdenum species, electrolysis in the IR thin-cell does not cleanly generate $CpFe(CO)_2^-$. Instead, the generation of an intermediate species is observed. Before generation of the first equivalent of $CpFe(CO)_2^-$ is complete, IR peaks for an unidentified species grow in at 1907 and 1961 cm^{-1}. After the starting compound is consumed, the remainder of the intermediate species is converted isosbestically to $CpFe(CO)_2^-$. We believe the intermediate species is the diphenyltin–iron anion, $CpFe(CO)_2SnPh_2^-$. This formulation is consistent with the observed infrared stretching frequencies. Table II compares the carbonyl stretching frequencies of each of the substituted metal carbonyls studied and includes the iron–tin intermediate under consideration. The ν_{CO} stretching frequencies for the $MSnPh_2(CH_3CN)_2^+$ species are an average of 30 cm^{-1} higher in energy relative to those for the isoelectronic triphenyltin adduct. In comparison, the ν_{CO} stretches for $CpFe(CO)_2SnPh_2^-$ are 32 cm^{-1} lower in energy. Thus, the shift in carbonyl stretching frequencies for the compounds $CpFe(CO)_2L$ follow the order $L = SnPh_2(CH_3CN)_2^+ > SnPh_3 > SnPh_2^-$, which is expected from electron-donation abilities. It is interesting to note that the anionic diphenyltin adduct is similar to the base-stabilized stannylene compounds discussed earlier, with the base occupied site in the stannylenes occupied by a lone pair of electrons in this case. The relatively small change in carbonyl stretching frequencies is consistent with this formulation. To our knowledge, no examples of transition-metal–diphenyltin anions of this type have previously been reported.

The generation of an intermediate species such as $CpFe(CO)_2SnPh_2^-$ leads us to believe that the reduction of $[CpFe(CO)_2]_2SnPh_2$ proceeds via a series of steps such as those proposed in eq 26 and 27. The first step is a net two-electron reduction

$$[CpFe(CO)_2]_2SnPh_2 + 2e^- \rightarrow CpFe(CO)_2^- + CpFe(CO)_2SnPh_2^- \quad (26)$$

$$CpFe(CO)_2SnPh_2^- \rightarrow CpFe(CO)_2^- + (1/n)(SnPh_2)_n \quad (27)$$

to yield 1 equiv of $CpFe(CO)_2^-$ and 1 equiv of the intermediate. The intermediate species than decomposes to give an additional equivalent of the iron anion and the tin oligomer. Since the final reduction products in this case are entirely analogous to those seen in the dimolybdenum case, it is tempting to propose an analogous scheme for its reduction. To be consistent with the spectral data, however, the decomposition of the molybdenum intermediate, $CpMo(CO)_3SnPh_2^-$, would have to be fast on the thin-cell bulk electrolysis time scale, since there is no spectral evidence for the generation of this species.

The reduction of $[Mn(CO)_5]_2SnPh_2$ is similar to the diiron and dimolybdenum cases in that the major product is the analogous organometallic anion fragment, $Mn(CO)_5^-$. However, the spectroelectrochemical data indicates neither generation of a well-defined intermediate species nor complete conversion of starting material to anion occurs. The intensity of signal due to the anion suggests that about 60% of the starting material is converted to the manganese pentacarbonyl anion. The additional compound(s) generated with the anion has a complex infrared spectrum and could not be identified.

Similar reduction chemistry was observed for $[Mn(CO)_5]_3SnPh$. The reduction peak current in the cyclic voltammogram for this compound is quite large relative to that for the oxidation peaks, and chronocoulometric data suggest that the process is a net four-electron process. Infrared spectral changes accompanying the reduction show that the major product is $Mn(CO)_5^-$ although additional species are generated. This chemistry is not explored further.

Conclusions

The electrochemistry and infrared spectroelectrochemistry of the compounds in the organotin–transition-metal series M_nSnPh_{4-n} (M = $CpMo(CO)_3$, $Mn(CO)_5$, $CpFe(CO)_2$; n = 1, 2) were studied in CH_3CN/TBAH. These compounds undergo net two-electron

(55) Cotton, F. A.; Wilkinson, G. *Advanced Inorganic Chemistry*, 5th ed.; Wiley: New York, 1988; pp 292–3.

oxidations, resulting in tin-metal bond cleavage. The oxidation products for the triphenyltin adducts are the solvent adducts of the transition-metal cation and the triphenyltin cation. When M = $Mn(CO)_5$, this oxidation is chemically reversible. Oxidation of the diphenyltin-bridged compounds results in cleavage of only one metal-tin bond, to give the metal cation and a base-stabilized stannylene cation. Analogous chemistry was observed for the related compounds $[Mn(CO)_5]_3SnPh$ and $[Mn(CO)_5]SnPh_2[CpFe(CO)_2]$. Experimental observations suggest that the latter compound is oxidized via an ECE mechanism.

Compounds in this series also undergo net one- or two-electron reductions and concomitant rupture of the tin-metal bonds. The triphenyltin adducts yield the monomeric metal anions and, in the diiron case, the triphenylstannate anion upon reduction. Reduction of the triphenyltin adduct of $CpMo(CO)_3$ yields Sn_2Ph_6 as the final tin product. The diphenyltin-bridged compounds are reduced to the transition-metal anions and an unreduced tin product, possibly $[SnPh_2]_n$. Infrared spectral data imply that reductions of the latter compounds proceed via terminal diphenyltin stannate anion adducts of the transition-metal moieties, e.g., $CpFe(CO)_2SnPh_2^-$.

The studies presented in this work demonstrate the utility of infrared spectroelectrochemistry toward the interpretation of non-Nernstian electrode processes. The unambiguous identification of electrogenerated species, as well as the ability to monitor their subsequent chemistry, is greatly facilitated via this technique.

Acknowledgment. J.P.B. thanks the University of Minnesota Graduate School for a Stanwood Johnson Memorial Fellowship and the University of Minnesota Chemistry Department for a departmental fellowship sponsored by 3M. The FT-IR spectrometer was purchased with funds provided by the NSF (Grant No. CHE 8509325). This work was funded in part by an additional grant from 3M.

Registry No. TBAH, 3109-63-5; $[CpMo(CO)_3]_2$, 60974-85-8; $[CpMo(CO)_3]SnPh_3$, 12100-85-5; $[CpMo(CO)_3]_2SnPh_2$, 12101-39-2; $[Mn(CO)_5]_2$, 10170-69-1; $[Mn(CO)_5]SnPh_3$, 14405-84-6; $[Mn(CO)_5]_2SnPh_2$, 15219-82-2; $[Mn(CO)_5]_3SnPh$, 15219-80-4; $[CpFe(CO)_2]_2$, 12154-95-9; $[CpFe(CO)_2]SnPh_3$, 12132-09-1; $[CpFe(CO)_2]_2SnPh_2$, 12100-78-6; $[Mn(CO)_5]SnPh_2[CpFe(CO)_2]$, 42867-99-2; $CpMo(CO)_3$, 12079-69-7; $Mn(CO)_5$, 15651-51-1; $CpFe(CO)_2$, 55009-40-0; $CpMo(CO)_3SnPh_2(CH_3CN)_2^+$, 129447-88-7; $Mn(CO)_5SnPh_2(CH_3CN)_2^+$, 129447-89-8; $CpFe(CO)_2SnPh_2(CH_3CN)_2^+$, 129447-90-1; $[CpMo(CO)_3]^-$, 12126-18-0; $[Mn(CO)_5]^-$, 14971-26-7; $[CpFe(CO)_2]^-$, 12107-09-4; CH_3CN, 75-05-8.

Supplementary Material Available: A table of double-step chronocoulometry data and diffusion coefficients, figures showing cyclic voltammograms of $[Mn(CO)_5]_2SnPh_2$, $[Mn(CO)_5]SnPh_2[CpFe(CO)_2]$, and $[CpFe(CO)_2]SnPh_2$, and plots of IR spectroelectrochemical data for $[Mn(CO)_5]_3SnPh$, $[CpMo(CO)_3]_2SnPh_2$, and $CpFe(CO)_2SnPh_3$ (7 pages). Ordering information is given on any current masthead page.

Contribution from the Institut für Anorganische Chemie, Universität Essen, D-4300 Essen, Federal Republic of Germany

Synthesis, Properties, and Structural Investigations of 1,3,2-Diazaborolidines and 2,3-Dihydro-1*H*-1,3,2-diazaboroles

Günter Schmid,* Michael Polk, and Roland Boese

Received February 14, 1990

A series of variously substituted 1,3,2-diazaborolidines have been prepared by different methods. 1,3-Diisopropyl-2-methyl-1,3,2-diazaborolidine (**1a**), 1,3-diethyl-2-methyl-1,3,2-diazaborolidine (**2a**), 1-ethyl-2,3-dimethyl-1,3,2-diazaborolidine (**3a**), and 1,2,3-trimethyl-1,3,2-diazaborolidine (**4a**) are formed from the corresponding lithiated ethylenediamines and CH_3BBr_2 in diethyl ether (method C). 2-Methyl-1-(trimethylsilyl)-1,3,2-diazaborolidine (**5a**), 1-*tert*-butyl-2-methyl-1,3,2-diazaborolidine (**6a**), and 1-isopropyl-2-methyl-1,3,2-diazaborolidine (**7a**) can be prepared either by method C, by method A, using the ethylenediamines and $H_3CB[N(CH_3)_2]_2$ to eliminate $HN(CH_3)_2$, or by method B, starting with CH_3BBr_2, NR_3, and the corresponding ethylenediamines. The unsaturated 2,3-dihydro-1*H*-1,3,2-diazaboroles **1b**–**7b** are synthesized by catalytic dehydrogenation in either liquid (**1b**–**3b**) or gaseous (**4b**–**7b**) state. Diazaboroles can act as 6-π-electron donors in $Cr(CO)_3$ complexes. **1b**–**4b** react with $(CH_3CN)_3Cr(CO)_3$ under various conditions to form the corresponding complexes **1c**–**4c**. The monosubstituted rings **5b**–**7b** are not suited to form stable $Cr(CO)_3$ complexes. One of the two rings in **8** can be combined with a $Cr(CO)_3$ fragment to give **9**. The yellow 1*H*-1,3,2-diazaborole–tricarbonylchromium complexes **1c**–**4c** decompose slowly at room temperature. 2,3-Dihydro-2-methyl-1,3-bis(trimethylsilyl)-1*H*-1,3,2-diazaborole (**10**) can be metalated at one N atom by $NaNH_2$ and K(O-*t*-Bu) to give the salts **11a** and **11b**. These alkali-metal derivatives can easily be protonated by HCl or CH_3OH to form the N–H derivative **5b**. X-ray structure analyses have been performed on the diazaborolidines **2a** and **4a** and on the diazaboroles **1b**, **2b**, **4b**, and **8**. The structures of **2a** and **4b** have been determined at two different temperatures. **1b**, **2b**, and **2a** crystallize in the monoclinic space groups $P2_1/n$, $P2_1/c$, and Cc, respectively. **4a** crystallizes hexagonally in the space group $P3_2$; **4b**, tetragonally in the space group $P4_3$. X–X-Difference electron densities of **4a**, **2a**, and **4b** show that the B–N bonds in the saturated compounds **4a** and **2a** possess remarkable double-bond character. The electron distribution in the 1,3,2-diazaborole **4b** corresponds with that in 6-π-electron systems.

Introduction

The formal substitution of a C=C unit in pyrrole by a B–N group leads to 2,3-dihydro-1*H*-1,3,2-diazaboroles:

pyrrole

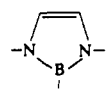

2,3-dihydro-1*H*-1,3,2-diazaborole

The first example of this class of compounds has been synthesized by a catalytic dehydrogenation of a saturated 1,3,2-diazaborolidine by Niedenzu et al. in 1973.[1]

Another simple, universally valid pathway was found by us in 1974, using borolium salts as intermediates:[2,3]

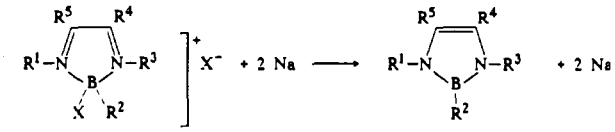

$R^1 = R^3$	R^2	$R^4 = R^5$	X
C_6H_5	CH_3	CH_3	Br
C_6H_5	CH_3	CH_3	Cl
C_6H_5	Br	CH_3	Br
C_6H_5	Cl	CH_3	Cl
$C(CH_3)_3$	CH_3	H	Br
$C(CH_3)_3$	Br	H	Br
$C(CH_3)_3$	Cl	H	Cl

1,3,2-Diazaboroles can act as 6-π-electron ligands in a few chromium complexes:[4,5]

(1) Merriam, J. S.; Niedenzu, K. *J. Organomet. Chem.* **1973**, *51*, C1.

0020-1669/90/1329-4421$02.50/0